Nuclear Medicine and Molecular Imaging in Nodal Staging and Surveillance of Ocular Melanoma: Case Reports and Review of the Literature

Kenneth S. Zurcher[1], Odette M. Houghton[2], Joanne F. Shen[2], Mahesh Seetharam[3], Michael C. Roarke[1], and Ming Yang[1]

[1]Department of Radiology, Mayo Clinic, Scottsdale, Arizona; [2]Department of Ophthalmology, Mayo Clinic, Scottsdale, Arizona; and [3]Department of Hematology/Oncology, Mayo Clinic, Scottsdale, Arizona

Ocular melanoma (OM) is a rare noncutaneous malignancy and consists of 2 different subtypes based on the anatomic location in the eye: uveal melanoma and conjunctival melanoma. Like cutaneous melanoma, OM benefits from nuclear medicine and molecular imaging in nodal staging and clinical management. Through the illustration of 2 distinctive cases, we aim to demonstrate the complementary roles of standard lymphoscintigraphy, advanced SPECT/CT, ^{18}F-FDG PET/CT, and ^{18}F-FDG PET/MRI in accurate nodal staging and surveillance of OM. We also review the epidemiology, existing staging guidelines, and management of uveal melanoma and conjunctival melanoma.

Key Words: conjunctival melanoma; ^{18}F-FDG/PET; lymphoscintigraphy; SPECT; uveal melanoma

Ocular melanoma (OM) represents the most common form of rare noncutaneous melanoma and the most common primary ocular tumor in adults (*1*). There are 2 subtypes of OM based on anatomic location in the eye: uveal melanoma (UM), which involves the choroid, retina, iris, or ciliary body and accounts for 95% of OM cases, and the rarer conjunctival melanoma (CM), which involves mainly the bulbar conjunctiva and comprises only about 5% of OM cases. The clinical manifestations of, and treatment approaches toward, OM vary between UM and CM, and accurate staging outside the eyes is crucial in the assessment of treatment response and surveillance (*2–4*).

Given the differences in lymphatic drainage and potential sites of metastases between UM and CM, distinct considerations must be made with regard to tumor staging strategies. Nuclear medicine and molecular imaging (i.e., ^{99m}Tc-sulfur colloid lymphoscintigraphy–guided sentinel lymph node biopsy [SLNB] and whole-body ^{18}F-FDG PET/CT) have proven of value in staging melanoma in the discovery of tracer-avid locoregional nodal and visceral metastases (*5–8*). Although limited data exist on the optimal imaging modality for staging CM, which has a lymphatic spread pattern similar to that of cutaneous melanoma, ^{99m}Tc-sulfur colloid lymphoscintigraphy and SPECT/CT-guided SLNB have emerged as valuable tools. Given the technical skill required for

subconjunctival radiotracer injection, these 2 tools have been used at only some specialized eye institutions (*9–12*). ^{18}F-FDG PET/MRI systems have become increasingly available and allow for combined whole-body molecular imaging and high-resolution, targeted, diagnostic MRI in a 1-stop imaging examination model. ^{18}F-FDG PET/MRI enables diagnosis of hepatic and brain metastasis and evaluation of tumor burden and assists in clinical management of OM (*13*).

In this study, we present 2 distinct cases to demonstrate the clinical utility of standard and advanced nuclear medicine imaging modalities in OM, followed by a review of OM epidemiology and existing guidelines on staging and management. Specifically, we aim to underscore the importance of ^{18}F-FDG PET/CT or ^{18}F-FDG PET/MRI in the staging or restaging of OM and the use of ^{99m}Tc-sulfur colloid lymphoscintigraphy and SPECT/CT in CM. This study complied with institutional review board policy.

CASES

Case 1

A 74-y-old man presented with visual changes in his left eye. On ophthalmologic examination, the patient was found to have retinal detachment with a large pigmented uveal mass, consistent with a diagnosis of ciliochoroidal melanoma. Staging CT and MRI of the liver demonstrated multiple hepatic lesions. Metastatic ciliochoroidal melanoma was confirmed after ultrasound-guided biopsy of a liver lesion revealed stage T4bN0M1 disease. The patient underwent γ-knife radiotherapy to the left-eye lesion and began systemic therapy with pembrolizumab. To evaluate response to therapy, ^{18}F-FDG PET/MRI was performed on a GE Healthcare Signa 3-T PET/MRI system. The customized PET/MRI protocol consisted of 2 parts. The first part was a whole-body ^{18}F-FDG PET/MRI survey scan with 370 MBq of ^{18}F-FDG injected intravenously, a 60-min uptake time, and 6–8 bed positions covering the whole body (an imaging time of ~4 min at each bed position). Simultaneous T1-weighted Dixon LAVA Flex (GE Healthcare; water, fat, in-phase, and out-of-phase) sequences were acquired for attenuation correction and localization. The second part was a focused contrast-enhanced liver MRI scan. The whole-body ^{18}F-FDG PET/MRI demonstrated a recurrent or residual tracer-avid primary left eye lesion on a survey scan, with progression of hepatic metastases (Fig. 1). The patient did not respond to chemotherapy and died 15 mo after the initial diagnosis of UM.

Case 2

A 64-y-old woman with a history of primary acquired melanosis (PAM) presented with a rapidly enlarging mobile lesion of the right
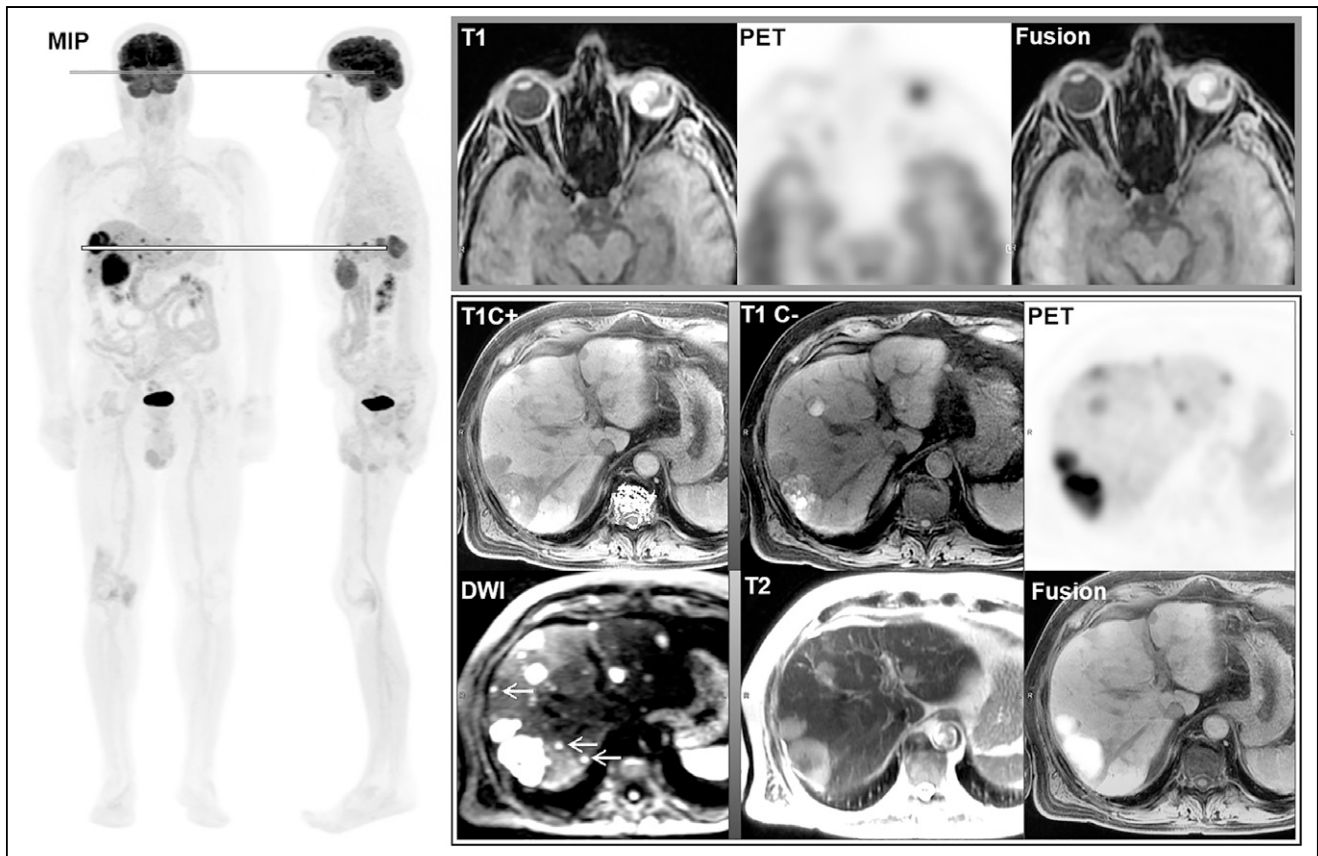
FIGURE 1. Whole-body ^{18}F-FDG PET/MRI study in surveillance of UM (case 1). Whole-body maximal-intensity-projection (MIP) images exhibit tracer-avid left eye lesion and numerous tracer-avid lesions in liver. Axial ^{18}F-FDG PET/MRI of left eye demonstrates high T1-signal lesion in left globe with increased tracer uptake, with SUV_{max} of 8.3 (top line on MIP image; top row of images). On representative layer of liver (bottom line on MIP image; bottom 2 rows of images), multiple liver lesions with variable low and high T1 signals show increased uptake, with SUV_{max} of 4.0–11.7. In addition, diffusion-weighted imaging (DWI) shows more small metastases with restricted diffusion (arrows) than does contrast-enhanced T1-weighted MRI (T1C+) or PET. T1C− = non–contrast-enhanced T1-weighted MRI; T2 = T2-weighted MRI. Color version of this figure is available as supplemental file at http://tech.snmjournals.org.

eye. On examination, a mobile pigmented lesion involving the right superior temporal conjunctiva was noted, with surrounding melanosis and without scleral invasion. The patient underwent excisional biopsy and cryotherapy. Pathologic examination revealed invasive bulbar CM with a 2.6-mm depth of invasion. Nasal and temporal margins were positive for residual PAM with atypia only. A further staging workup was performed, including whole-body ^{18}F-FDG PET/CT (same dosage and uptake time as for whole-body ^{18}F-FDG PET/MRI) and MRI of the brain and neck, both of which were negative for a recurrent lesion or metastatic disease. Lymphoscintigraphy for the purposes of SLNB was also performed. Subconjunctival radiotracer injection was performed by an ophthalmologist with a valid authorized-user status. In detail, 4% lidocaine was topically administered with a cotton tip applicator to the injection site of the right eye following a dedicated sterile preparation protocol. With the patient's eyelids manually held open by the ophthalmologist, the patient was instructed to look in the opposite direction from the injection site, and two 0.2-mL aliquots of normal saline containing 11.1 MBq of ^{99m}Tc-filtered sulfur colloid were successfully injected in the subconjunctival space in separate locations in the area of the excised melanoma. Dynamic and static planar scintigraphy images of the head and neck were obtained, followed by SPECT/CT images,

to localize the sentinel node. Both planar and SPECT images identified a right parotid sentinel node, which was resected through a superficial parotidectomy and was negative for metastasis on final pathologic examination (Fig. 2). The disease was staged as T1cN0M0. The patient remained negative for tumor recurrence or metastasis on repeated biopsy and multimodality image studies,
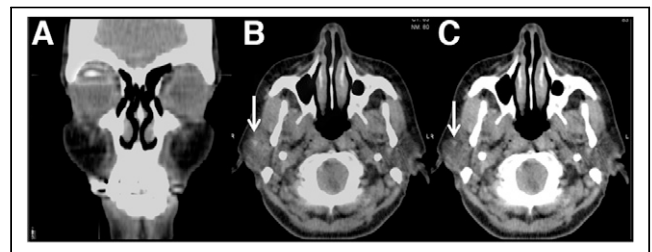

FIGURE 2. ^{99m}Tc-filtered sulfur colloid SPECT/CT (case 2). (A) Coronal PET/MR image demonstrating successful radiotracer injection to right-eye subconjunctival region by ophthalmologist. (B) Axial PET/MR image. (C) Axial low-dose CT image. Tiny sentinel lymph node (arrows) was identified in right fossa of parotid gland. Node was negative for metastasis on biopsy. Color version of this figure is available as supplemental file at http://tech. snmjournals.org.
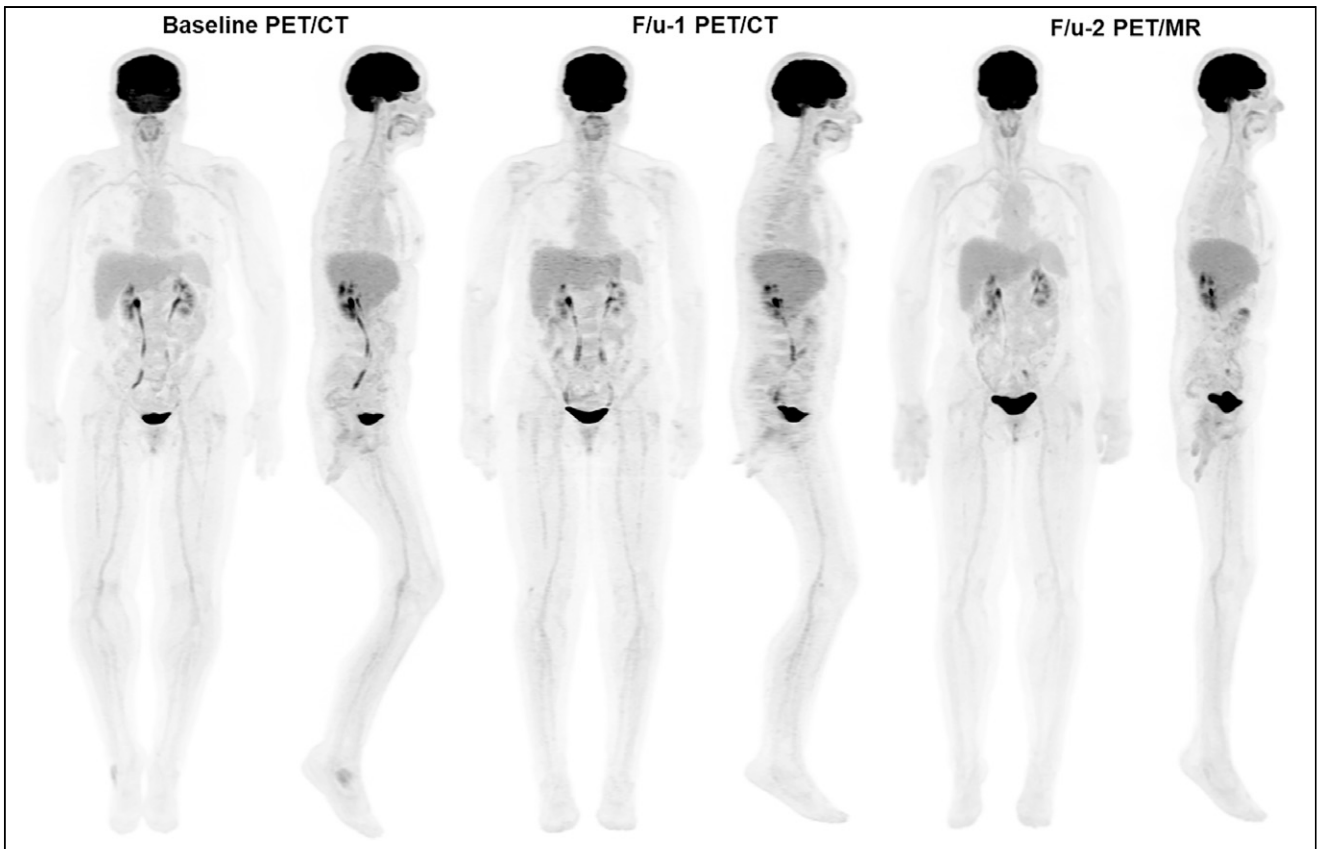
FIGURE 3. Whole-body maximum-intensity-projection ^{18}F-FDG PET/CT and ^{18}F-FDG PET/MRI in surveillance of CM (case 2). Consecutive anterior and right lateral views do not demonstrate hypermetabolic metastasis or recurrence at baseline or at the first (12 mo) or second (16 mo) follow-up (F/u-1 and F/u-2, respectively).
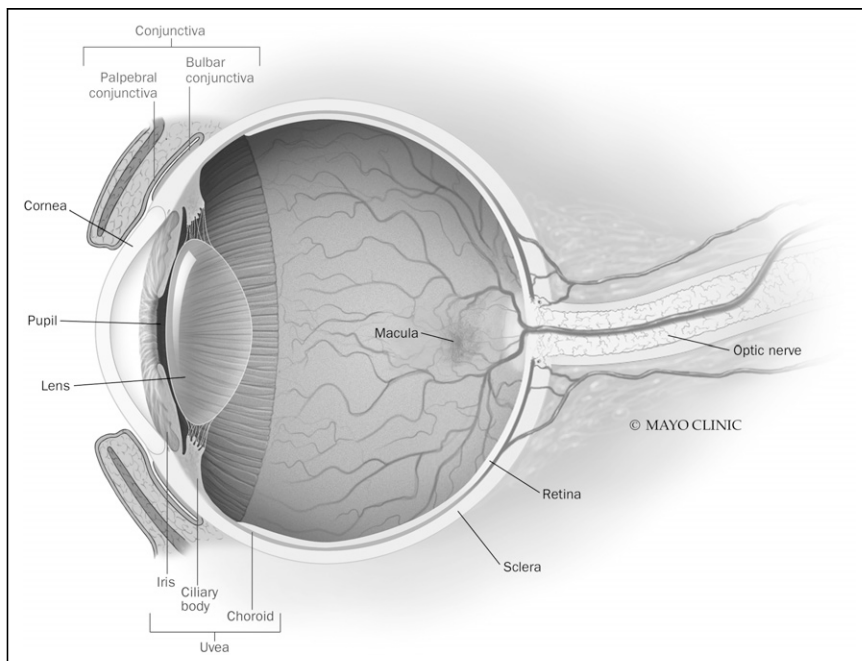

FIGURE 4. Illustration of eye anatomy. UM occurs at iris, ciliary body, and choroid. CM occurs at palpebral and bulbar conjunctiva. (Reprinted with permission of (*38*).) Color version of this figure is available as supplemental file at http://tech.snmjournals.org.

including whole-body ^{18}F-FDG PET/CT and ^{18}F-FDG PET/MRI (Fig. 3).

DISCUSSION

OM is a rare type of noncutaneous melanoma and the second most common melanoma after cutaneous melanoma (*1*). On the basis of its anatomic location, OM is categorized as UM or CM (Fig. 4). There are distinctive differences in epidemiology, pathophysiology, and clinical management between these 2 subtypes. Accurate staging and appropriate clinical surveillance may guide clinical management and ultimately improve prognosis in UM and CM, similarly to their cutaneous melanoma counterpart. From SLNB to whole-body ^{18}F-FDG PET/CT, nuclear medicine and molecular imaging have a well-established role in staging and surveillance of cutaneous melanoma. Given the complex anatomy of the eye and the rarity of OM, we present these 2 cases to demonstrate that the variety of nuclear medicine and molecular imaging modalities provides excellent imaging tools in staging and surveillance of OM.

UM

Epidemiology and Pathophysiology. UM represents the most common primary intraocular malignancy in adults, with a mean age-adjusted incidence of 5.1 per million population (*1,14–16*). On the basis of Surveillance, Epidemiology, and End Results data collected in the United States between 1973 and 2008, UM represented approximately 3.1% of all melanoma cases, with 5- and 15-y survival rates of 81.6% and 45%, respectively (*15,16*). UM develops from melanocytes along the uveal tract and most frequently arises from the choroid (85%), with retinal, iris, and ciliary body involvement comprising the remainder of cases (*14,17*). Increased rates of UM are seen in white populations.

Staging. Because of a relative lack of lymphatics within the eye, metastatic spread of UM occurs predominantly in a hematogenous manner. Although metastases can be found in several organ systems, UM demonstrates a notorious propensity for liver metastasis. Although this mechanism is not well understood, an estimated 71%–95% of patients with metastatic disease demonstrate hepatic lesions; other metastatic sites include bone, lung, skin, and other organ systems (*14,18,19*).

Staging of OM is guided by the American Joint Committee on Cancer, with imaging playing a vital role in identifying metastatic disease (*16*). Consensus-based guidelines on staging workup of UM were proposed by Weis et al. (*16*) in 2016 and recommend that one of the following be obtained: CT of the chest and abdomen (liver protocol for abdomen), whole-body ^{18}F-FDG PET/CT, or liver MRI with chest CT.

Recent studies have highlighted the sensitivity and positive predictive value of both ^{18}F-FDG PET/CT and MRI in assessing metastatic UM. A 2012 study by Freton et al. (*20*) highlighted ^{18}F-FDG PET/CT as an effective screening modality for hepatic and extrahepatic metastasis, with a 100% positive predictive value. Of 333 consecutive patients with UM who underwent screening with ^{18}F-FDG PET/CT, 7 demonstrated biopsy-proven liver metastases, and 2 of those 7 (29%) had multiorgan involvement. In a 2005 study by Kurli et al. (*19*), 20 patients with suspected metastatic UM underwent ^{18}F-FDG PET/CT to identify metastatic disease. Of 8 patients positive for metastasis, 8 (100%) demonstrated liver metastasis and 6 (75%) showed multiorgan involvement, resulting in a sensitivity of 100%. Klingenstein et al. (*21*), in 2010, further established ^{18}F-FDG PET/CT as an effective tool in imaging staging and follow-up of metastatic UM.

In specifically determining the presence of isolated hepatic metastatic disease, a 2010 study by Servois et al. (*22*) reported the sensitivity and positive predictive value of liver MRI to be 67% and 95%, respectively, compared with 41% and 100% for ^{18}F-FDG PET/CT. This increased sensitivity of MRI over ^{18}F-FDG PET/CT in detecting liver lesions was further corroborated in a 2012 study by Orcurto et al. (*23*), in which MRI outweighed ^{18}F-FDG PET/CT in detecting small lesions (<1.2 cm). Importantly, in that study, ^{18}F-FDG PET/CT identified at least one metastatic liver lesion per patient as well as changes in ^{18}F-FDG uptake not related to size change, suggesting a potential role in determining early therapy response.

Although a single optimal imaging modality has not yet been determined in the staging of UM, benefits exist for both ^{18}F-FDG PET/CT (identifying extrahepatic disease with good sensitivity and positive predictive value for hepatic lesions) and MRI (improved sensitivity for identifying hepatic lesions). In case 1, ^{18}F-FDG PET/MRI was chosen as the optimal surveillance modality, which demonstrated excellent performance in delineating both the primary lesion and the hepatic metastases in the advantageous 1-stop imaging pattern. The hybrid diagnostic liver ^{18}F-FDG PET/MRI demonstrated its unique advantage in combining morphologic and molecular imaging information in the diagnosis of liver metastasis in melanoma. If available or feasible, ^{18}F-FDG PET/MRI may represent an alternative that combines the described advantages of both modalities, with a reduced radiation dose compared with whole-body ^{18}F-FDG PET/CT.

Management. Management of UM is highly specialized and requires multidisciplinary support. With regard to surgical management, enucleation remains the preferred treatment for lesions more than 10 mm thick or more than 18 mm in diameter (*16*). Local resection can be considered in select ciliary body or iris lesions. Lesions best suited for brachytherapy include those less than 10 mm thick and less than 18 mm in maximal diameter, as well as high-risk indeterminate lesions.

The appropriate imaging surveillance strategy for patients with metastatic UM remains to be fully established. However, annual follow-up with ^{18}F-FDG PET/CT or liver MRI, or with liver ultrasonography and chest radiography, is recommended. Although a prospective study of 188 high-risk UM patients showed that semiannual liver MRI detected metastases in 92% of patients before symptoms manifested, whether such a regimen has a survival benefit remains to be established (*24*).

CM

Epidemiology and Pathophysiology. CM represents a considerably rarer entity than UM, occurring approximately one fortieth as often, with an estimated annual incidence of 0.2–0.8 cases per million (*25–29*). CM is predominantly seen in middle-aged to older white populations, without a definite sex predilection. Five- and 8-y mortalities have been most recently estimated at 7% and 13%, respectively (*30*). Although risk factors commonly associated with cutaneous melanoma have not been demonstrated in CM (e.g., family history, ultraviolet light exposure, or fair skin and hair), an association between PAM and CM has been well established. Of CM cases, 57%–76% are thought to be attributable to PAM—with PAM with severe atypia transforming into CM at a high frequency (*30,31*). CM results from malignant proliferation of melanocytes—specifically from the conjunctiva. Anatomically, the conjunctiva represents a clear mucous membrane that lines the posterior surface of the eyelids (palpebral conjunctiva), the anterior portions of the globe, and the superior and inferior fornices (bulbar and forniceal conjunctiva, respectively) (*25*). However, there is no particular quadrant prediction, with the following quadrant incidence ranges reported: 16%–34% in the superior quadrant, 22%–39% in the inferior quadrant, 17%–34% in the nasal quadrant, and 26%–63% in the temporal quadrant (*30,32*).

Staging. Because the conjunctiva is supplied by both blood vessels and lymphatics, metastatic spread can occur hematogenously or via lymphatic drainage to regional lymph nodes. Initial lymphatic spread is estimated to occur in up to 41%–62% of patients, with distant metastases in the absence of local nodal involvement occurring in 26%–50% (*3,30,33*). Reported risk factors for regional nodal spread include nonlimbal location, tumor thickness greater than 2 mm, large basal diameter, positive resection margins, and orbital extension (*34*). The lymphatic spread of CM seems to be associated with the location of the primary tumor, with nasal conjunctiva appearing to drain to the submandibular lymph nodes (9%) whereas tumors of the rest of the conjunctiva drain primarily to the

preauricular nodes (73%) and deep cervical lymph nodes (18%) (*3*). Currently, no strict imaging guidelines exist for systemic staging workup or restaging of CM (*4,31*). Existing recommendations include CT or MRI of the brain, chest, and abdomen/liver or ^{18}F-FDG PET/CT. In contrast to UM, a paucity of data exists assessing the utility of ^{18}F-FDG PET/CT in CM. The largest case series was reported by Kurli et al. (*35*), who investigated the performance of ^{18}F-FDG PET/CT in 14 CM patients: 7 for peroperative staging and 7 for restaging after treatment (surgical removal with adjuvant cryotherapy or chemotherapy). Among the small cohort of patients, one (T4 stage) had multisite distant metastases, with involvement of the liver, lung, peritoneal cavity, lumbar spine, and other sites. The remaining 13 patients (T3 stage) were negative for either locoregional or distant metastasis. This study indicated a limited role for ^{18}F-FDG PET/CT in initial T and N staging but value for restaging of CM. Damian et al. reported a case presenting with a hypermetabolic primary left-eye CM lesion and an ipsilateral preauricular node on restaging ^{18}F-FDG PET/CT, without evidence of distant metastasis (*36*).

Because of the similarity in the pattern of lymphatic spread between CM and cutaneous melanoma, lymphoscintigraphy with SLNB has arisen as a safe and viable staging tool in the last 1–2 decades and has been supported in several small case series (*11,34,36*). Preoperative SLNB allows for potential detection of otherwise clinically undetectable systemic spread and is performed during or after removal of the primary lesion (*31*). The success of SLNB requires a sophisticated subconjunctival injection of filtered [99mTc]-sulfur colloid near the existing tumor or site of resection at the nuclear medicine laboratory (*37*). Dynamic planar images are obtained with a γ-camera to identify a sentinel lymph node. The skin is marked in this region, with use of SPECT/CT for further localization. Intraoperatively, a handheld γ-probe and methylene blue injection are also used to localize the sentinel node, followed by surgical dissection, excision, and histologic processing.

Ultimately, further trials are required to fully identify the role and survival benefit of lymphoscintigraphy with SLNB in this population. Given the rarity of CM, existing data remain limited, with a cohort of 18 patients from Cohen et al. (*34*) remaining the largest studied population.

Management. Again, because of the rarity of CM, management of this malignancy is based on case reports and series. The current standard of care includes wide local excision with double freeze–thaw cryotherapy to the resection margins (*4,31*). Enucleation may be required in advanced cases in which wide local excision is not feasible. Topical chemotherapy and brachytherapy have been explored as adjuvant therapy. Unfortunately, 5-y recurrence rates are high, currently estimated at 36%–45% after surgical resection (*31*). Like UM, CM currently has no optimal or well-researched method of imaging surveillance for restaging, with ^{18}F-FDG PET/CT often being used.

CONCLUSION

Nuclear medicine and molecular imaging have an established role in the staging and surveillance of OM. Because of differences in metastatic pathways between UM and CM, imaging strategies for both entities also differ. In patients with UM, whole-body ^{18}F-FDG PET/CT may represent mainstays of initial staging and surveillance. The role of emerging hybrid ^{18}F-FDG PET/MRI is promising, especially in the diagnosis and assessment of metastasis in the liver and brain, but it is limited by lack of availability and needs to be better defined

by greater clinical application. Data on the staging and surveillance of CM remain sparse and are based on limited case series. Since CM may spread to locoregional lymph nodes via the lymphatic drainage channel, there is a rationale for performing SLNB and SPECT/CT in the staging of CM to predict recurrence and survival. Collaboration with ophthalmology at a clinical nuclear medicine practice is crucial to successfully perform the sophisticated subconjunctival radiotracer injection.

DISCLOSURE

No potential conflict of interest relevant to this article was reported.

REFERENCES

1. McLaughlin CC, Wu XC, Jemal A, Martin HJ, Roche LM, Chen VW. Incidence of noncutaneous melanomas in the U.S. *Cancer.* 2005;103:1000–1007.
2. Aronow ME, Topham AK, Singh AD. Uveal melanoma: 5-year update on incidence, treatment, and survival (SEER 1973-2013). *Ocul Oncol Pathol.* 2018;4:145–151.
3. Esmaeli B, Wang X, Youssef A, Gershenwald JE. Patterns of regional and distant metastasis in patients with conjunctival melanoma: experience at a cancer center over four decades. *Ophthalmology.* 2001;108:2101–2105.
4. Vora GK, Demirci H, Marr B, Mruthyunjaya P. Advances in the management of conjunctival melanoma. *Surv Ophthalmol.* 2017;62:26–42.
5. Fuster D, Chiang S, Johnson G, Schuchter LM, Zhuang H, Alavi A. Is ^{18}F-FDG PET more accurate than standard diagnostic procedures in the detection of suspected recurrent melanoma? *J Nucl Med.* 2004;45:1323–1327.
6. Morton DL, Wen DR, Wong JH, et al. Technical details of intraoperative lymphatic mapping for early stage melanoma. *Arch Surg.* 1992;127:392–399.
7. Steinert HC, Huch Böni RA, Buck A, et al. Malignant melanoma: staging with whole-body positron emission tomography and 2-[F-18]-fluoro-2-deoxy-D-glucose. *Radiology.* 1995;195:705–709.
8. Wong SL, Faries MB, Kennedy EB, et al. Sentinel lymph node biopsy and management of regional lymph nodes in melanoma: American Society of Clinical Oncology and Society of Surgical Oncology clinical practice guideline update. *Ann Surg Oncol.* 2018;25:356–377.
9. Balasubramanya R, Selvarajan SK, Cox M, et al. Imaging of ocular melanoma metastasis. *Br J Radiol.* 2016;89:20160092.
10. Esmaeli B. Sentinel lymph node mapping for patients with cutaneous and conjunctival malignant melanoma. *Ophthal Plast Reconstr Surg.* 2000;16:170–172.
11. Esmaeli B, Eicher S, Popp J, Delpassand E, Prieto VG, Gershenwald JE. Sentinel lymph node biopsy for conjunctival melanoma. *Ophthal Plast Reconstr Surg.* 2001;17:436–442.
12. Reddy S, Kurli M, Tena LB, Finger PT. PET/CT imaging: detection of choroidal melanoma. *Br J Ophthalmol.* 2005;89:1265–1269.
13. Buchbender C, Heusner TA, Lauenstein TC, Bockisch A, Antoch G. Oncologic PET/MRI, part 2: bone tumors, soft-tissue tumors, melanoma, and lymphoma. *J Nucl Med.* 2012;53:1244–1252.
14. Kalemaki MS, Karantanas AH, Exarchos D, et al. PET/CT and PET/MRI in ophthalmic oncology. *Int J Oncol.* 2020;56:417–429.
15. Singh AD, Turell ME, Topham AK. Uveal melanoma: trends in incidence, treatment, and survival. *Ophthalmology.* 2011;118:1881–1885.
16. Weis E, Salopek TG, McKinnon JG, et al. Management of uveal melanoma: a consensus-based provincial clinical practice guideline. *Curr Oncol.* 2016;23:e57–e64.
17. Vora GK, Demirci H, Marr B, Mruthyunjaya P. Advances in the management of conjunctival melanoma. *Surv Ophthalmol.* 2017;62:26–42.
18. Bakalian S, Marshall JC, Logan P, et al. Molecular pathways mediating liver metastasis in patients with uveal melanoma. *Clin Cancer Res.* 2008;14:951–956.
19. Kurli M, Reddy S, Tena LB, Pavlick AC, Finger PT. Whole body positron emission tomography/computed tomography staging of metastatic choroidal melanoma. *Am J Ophthalmol.* 2005;140:193–199.
20. Freton A, Chin KJ, Raut R, Tena LB, Kivelä T, Finger PT. Initial PET/CT staging for choroidal melanoma: AJCC correlation and second nonocular primaries in 333 patients. *Eur J Ophthalmol.* 2012;22:236–243.
21. Klingenstein A, Haug AR, Nentwich MM, Tiling R, Schaller UC. Whole-body F-18-fluoro-2-deoxyglucose positron emission tomography/computed tomography imaging in the follow-up of metastatic uveal melanoma. *Melanoma Res.* 2010;20:511–516.

22. Servois V, Mariani P, Malhaire C, Petras S, Piperno-Neumann S, Plancher C. Preoperative staging of liver metastases from uveal melanoma by magnetic resonance imaging (MRI) and fluorodeoxyglucose-positron emission. *Eur J Surg Oncol.* 2010;36:189–194.

23. Orcurto V, Denys A, Voelter V, et al. ^{18}F-fluorodeoxyglucose positron emission tomography/computed tomography and magnetic resonance imaging in patients with liver metastases from uveal melanoma: results from a pilot study. *Melanoma Res.* 2012;22:63–69.

24. Marshall E, Romaniuk C, Ghaneh P, et al. MRI in the detection of hepatic metastases from high-risk uveal melanoma: a prospective study in 188 patients. *Br J Ophthalmol.* 2013;97:159–163.

25. Brownstein S. Malignant melanoma of the conjunctiva. *Cancer Control.* 2004;11:310–316.

26. Shildkrot Y, Wilson MW. Conjunctival melanoma: pitfalls and dilemmas in management. *Curr Opin Ophthalmol.* 2010;21:380–386.

27. Triay E, Bergman L, Nilsson B, All-Ericsson C, Seregard S. Time trends in the incidence of conjunctival melanoma in Sweden. *Br J Ophthalmol.* 2009;93:1524–1528.

28. Tuomaala S, Eskelin S, Tarkkanen A, Kivelä T. Population-based assessment of clinical characteristics predicting outcome of conjunctival melanoma in whites. *Invest Ophthalmol Vis Sci.* 2002;43:3399–3408.

29. Yu GP, Hu DN, McCormick S, Finger PT. Conjunctival melanoma: is it increasing in the United States? *Am J Ophthalmol.* 2003;135:800–806.

30. Shields CL, Shields JA, Gunduz K, et al. Conjunctival melanoma: risk factors for recurrence, exenteration, metastasis, and death in 150 consecutive patients. *Arch Ophthalmol.* 2000;118:1497–1507.

31. Wong JR, Nanjp AA, Galor A, Karp CL. Management of conjunctival malignant melanoma: a review and update. *Expert Rev Ophthalmol.* 2014;9:185–204.

32. Shields CL, Markowitz JS, Belinsky I, et al. Conjunctival melanoma: outcomes based on tumor origin in 382 consecutive cases. *Ophthalmology.* 2011;118:389–395.e1-2

33. Tuomaala S, Kivelä T. Metastatic pattern and survival in disseminated conjunctival melanoma: implications for sentinel lymph node biopsy. *Ophthalmology.* 2004;111:816–821.

34. Cohen VML, Tsimpida M, Hungerford JL, Jan H, Cerio R, Moir G. Prospective study of sentinel lymph node biopsy for conjunctival melanoma. *Br J Ophthalmol.* 2013;97:1525–1529.

35. Kurli M, Chin K, Finger PT. Whole-body 18 FDG PET/CT imaging for lymph node and metastatic staging of conjunctival melanoma. *Br J Ophthalmol.* 2008;92:479–482.

36. Damian A, Gaudiano J, Engler H, Alonso O. ^{18}F-FDG PET-CT for staging of conjunctival melanoma. *World J Nucl Med.* 2013;12:45–47.

37. Wainstein AJ, Drummond-Lage AP, Kansaon MJ, et al. Sentinel lymph node biopsy for conjunctival malignant melanoma: surgical techniques. *Clin Ophthalmol.* 2014;9:1–6.

38. Bakri SJ, ed. *Mayo Clinic Guide to Better Vision.* Mayo Foundation for Medical Education and Research; 2014:11.